Local Observation of Field Polarity Dependent Flux Pinning by Magnetic Dipoles

M. J. Van Bael, J. Bekaert, K. Temst, L. Van Look, V. V. Moshchalkov, and Y. Bruynseraede
Laboratorium voor Vaste-Stoffysica en Magnetisme, K. U. Leuven, Celestijnenlaan 200D, B-3001 Leuven, Belgium

G. D. Howells, A. N. Grigorenko, and S. J. Bending
Department of Physics, University of Bath, Claverton Down, Bath BA2 7AY, United Kingdom

G. Borghs
Inter-University Micro-Electronics Center (IMEC vzw), Kapeldreef 75, B-3001 Leuven, Belgium
(Received 12 July 1999)

A scanning Hall probe microscope is used to study flux pinning in a thin superconducting Pb film covering a square array of single-domain Co dots with in-plane magnetization. We show that single flux quanta of opposite sign thread the superconducting film below T_c at the opposite poles of these dipoles. Depending on the polarity of the applied field, flux lines are attracted to a specific pole of the dipoles, due to the direct interaction with the vortexlike structures induced by the local stray field.

DOI: 10.1103/PhysRevLett.86.155 PACS numbers: 74.60.Ge, 07.79.–v, 74.76.Db

Over the last decade, advances in microfabrication have allowed the production of superconducting (SC) samples with ordered artificial pinning arrays, e.g., an antidot lattice in a thin film [1–3]. These artificial pinning arrays give rise to a strong enhancement of the bulk magnetization and critical current and have been successfully used to gain insight into the microscopic nature of pinning. Commensurability effects between the periodic flux line (FL) lattice and ordered pinning arrays have also been studied, and stable FL configurations have been imaged directly using Lorentz microscopy [4]. More recently, regular arrays of *ferromagnetic dots* have been explored where additional pinning contributions arise due to the magnetic nature of the pinning centers [5–8]. While macroscopic commensurability effects have already been demonstrated in such systems, insight into the *microscopic origin* of these pinning phenomena is still lacking. The system studied in this Letter is a type-II superconducting Pb film deposited on top of a lattice of magnetic dipoles consisting of single-domain Co dots with in-plane magnetization. Using scanning Hall probe microscopy (SHPM), we directly visualize the FLs simultaneously with the local stray fields of the magnetic pinning centers. We show that the FLs are preferentially pinned at one specific side of a dipole, determined by the sign of the applied field, giving a direct indication of the microscopic interaction mechanism of FLs with these *magnetic* pinning centers.

Square lattices (period $a = 1.5\ \mu$m) of rectangular submicron polycrystalline magnetic dots, consisting of a Au(7.5 nm)/Co(20 nm)/Au(7.5 nm) trilayer, are fabricated by electron-beam lithography and molecular beam deposition [7]. The dots have lateral dimensions of 540 nm (easy axis) $\times$ 360 nm. Magnetic force microscopy (MFM) at room temperature reveals a multidomain as-grown state. After magnetization along the easy axis all dots are in a single-domain remanent state [7]. The dot array was covered with a 50 nm SC Pb film, a protective Ge layer (20 nm), and a 10 nm Au layer for the scanning tunneling microscopy (STM) distance control of the SHPM. The SHPM used is a modified commercial low temperature STM where the tunneling tip is replaced by a Hall probe, defined in a GaAs/AlGaAs heterostructure chip at the intersection of two 200 nm wide wires [9,10]. The Hall sensor was about 200–300 nm above the sample for the presented scans.

We will describe measurements above and below the SC critical temperature of the Pb film ($T_c = 7.16$ K) with an applied field (B) normal to the sample plane. Prior to all measurements, all dots are aligned in a single-domain state. Earlier characterization of the same sample by AFM and MFM showed a homogeneous period and very uniform dimensions and magnetic contrast of all dots [7]. Figure 1

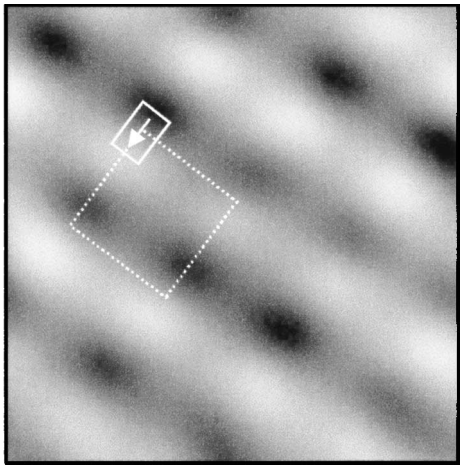

FIG. 1. SHPM image of the square lattice of single-domain Co dots at $B = 0$ and $T = 77$ K. The gray scale represents the magnitude of the perpendicular component of the local stray field b (bright: $b > 0$, dark: $b < 0$). As a guide to the eye, the unit cell of the dot array (dotted line) and the position of one dot (full line) are also indicated.

shows a SHPM image of a region near the center of the sample at $B = 0$ and temperature $T = 77$ K. The dipole stray fields characteristic for an ordered array of single-domain particles are clearly visible. Minor nonuniformities in contrast between different dots can partly be attributed to a small tilt angle between sample and scanning planes. Moreover, since high spatial frequencies in the image are damped exponentially with increasing sample-sensor spacing, small differences in scan height can lead to significant changes in image contrast.

Upon cooling through T_c, the flux created at both poles of the magnetic dots must obey fluxoid quantization. This means that screening currents are locally generated in the SC film in order to quantize the total flux at each pole to the nearest integer multiple of ϕ_0, with ϕ_0 the SC flux quantum. Unless the dot length is much smaller than the penetration depth $\lambda(T)$, both poles will be quantized separately. If the stray field of both poles creates a (positive or negative) flux between $|n - \frac{1}{2}|\phi_0$ and $|n|\phi_0$ (with n integer), local currents around each pole will *add* a small amount of flux to create a fluxoid of exactly $|n|\phi_0$ at one pole and $-|n|\phi_0$ at the opposite pole of the dot. In the case that the magnitude of flux at each pole is between $|n|\phi_0$ and $|n + \frac{1}{2}|\phi_0$, screening currents circulate in the opposite direction and will effectively *lower* the flux to create a fluxoid of $\pm|n|\phi_0$ at the opposite poles. (The actual microscopic distribution of the screening currents should be determined by minimizing the free energy of the system [11].) To investigate this effect, the magnitude of the dipole fields that penetrate the SC film is probed as a function of T in the close vicinity of T_c. Figure 2 shows the peak-to-valley difference between the measured field value above the opposite poles of the magnetic dots (averaged over four dots in a 3×3 μm^2 area) in zero applied field as a function of T. As T drops below T_c,

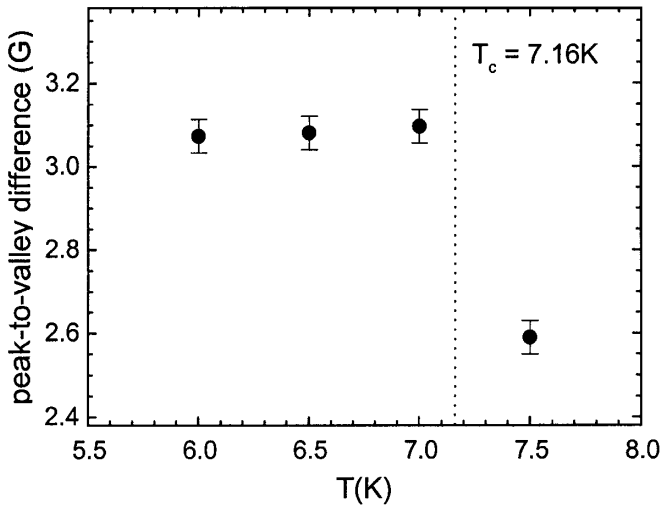

FIG. 2. Average peak-to-valley difference of the measured local field above the opposite poles of the Co dots as function of temperature. T_c is indicated by the dotted line.

a sudden increase of this field contrast is observed. This sudden jump indicates the appearance of screening currents in the SC film, which slightly *increase* the total flux at each pole to satisfy fluxoid quantization. This result implies that in our case, the stray field threading the Pb film at each pole corresponds to a flux slightly less than an integer multiple of ϕ_0. From this result only, it is not possible to determine the number of flux quanta generated at the poles of the dots. However, later in this Letter we give evidence that only a single flux quantum is formed at each pole, which would be a realistic estimate of the stray field of the dots. Based on these results, we infer that below T_c each magnetic dot establishes a kind of pinned "vortex-antivortex pair," with opposite screening currents at the two poles that are only a fraction of those of a normal vortex or antivortex. Since in our case a small amount of flux is *added* to satisfy fluxoid quantization, the rotation direction of the screening currents of the dot-induced vortex (antivortex) is the same as that of a normal vortex (antivortex), but the current magnitude is significantly lower. We will therefore also use the terms "vortex" and "antivortex" for these flux quanta generated at the poles of the dots.

From earlier work on the same system it is known that these magnetic dots act as strong pinning centers for the flux lines in a perpendicular applied magnetic field [7]. There are several possible sources of pinning in these samples, e.g., corrugations of the Pb film on top of the dots and local weakening of the SC order parameter by the stray field of the dots. To investigate how additional FLs interact with the magnetic dipoles, SHPM experiments are performed in an applied magnetic field. Since the dipole fields and the FLs are imaged simultaneously, the position of an individual FL with respect to a magnetic dot can be determined. (Because of the reduction of the range of the piezoelectric tube scanner at low temperatures, the scan range is limited to about 3.2×3.2 μm^2.) The SHPM results at $T = 6$ K $< T_c$ after field cooling at $B/B_1 = -\frac{1}{2}$ and $+\frac{1}{2}$ are shown in Figs. 3(b) and 3(f), respectively. The first matching field B_1 is defined as the applied field at which exactly one flux quantum ϕ_0 is present per unit cell of the pinning array, i.e., $B_1 \equiv \phi_0/a^2 = 9.2$ G. The contributions of the dipoles at the same location of the sample (at $T = 7.5$ K $> T_c$, $B/B_1 = -\frac{1}{2}$) are displayed in Fig. 3(a). Below T_c, disregarding the FLs generated by the applied field, an integer number of flux quanta penetrates the SC film at both poles of each dot. After additional FLs have penetrated the Pb film at $B/B_1 = -\frac{1}{2}$, the positive (bright) poles of some of the dots have disappeared [see Fig. 3(b)], which indicates that a negative FL is added on this pole. This is schematically indicated in Fig. 3(c); at the position of the disappeared bright poles a negative FL (black circle) is trapped. In order to identify the FL locations, we subtract the dipole contribution at $T = 7.5$ K $> T_c$ [Fig. 3(a)] from the image at $T < T_c$ [Fig. 3(b)] to obtain Fig. 3(d), containing mainly information about the additional FLs. Although this subtraction is

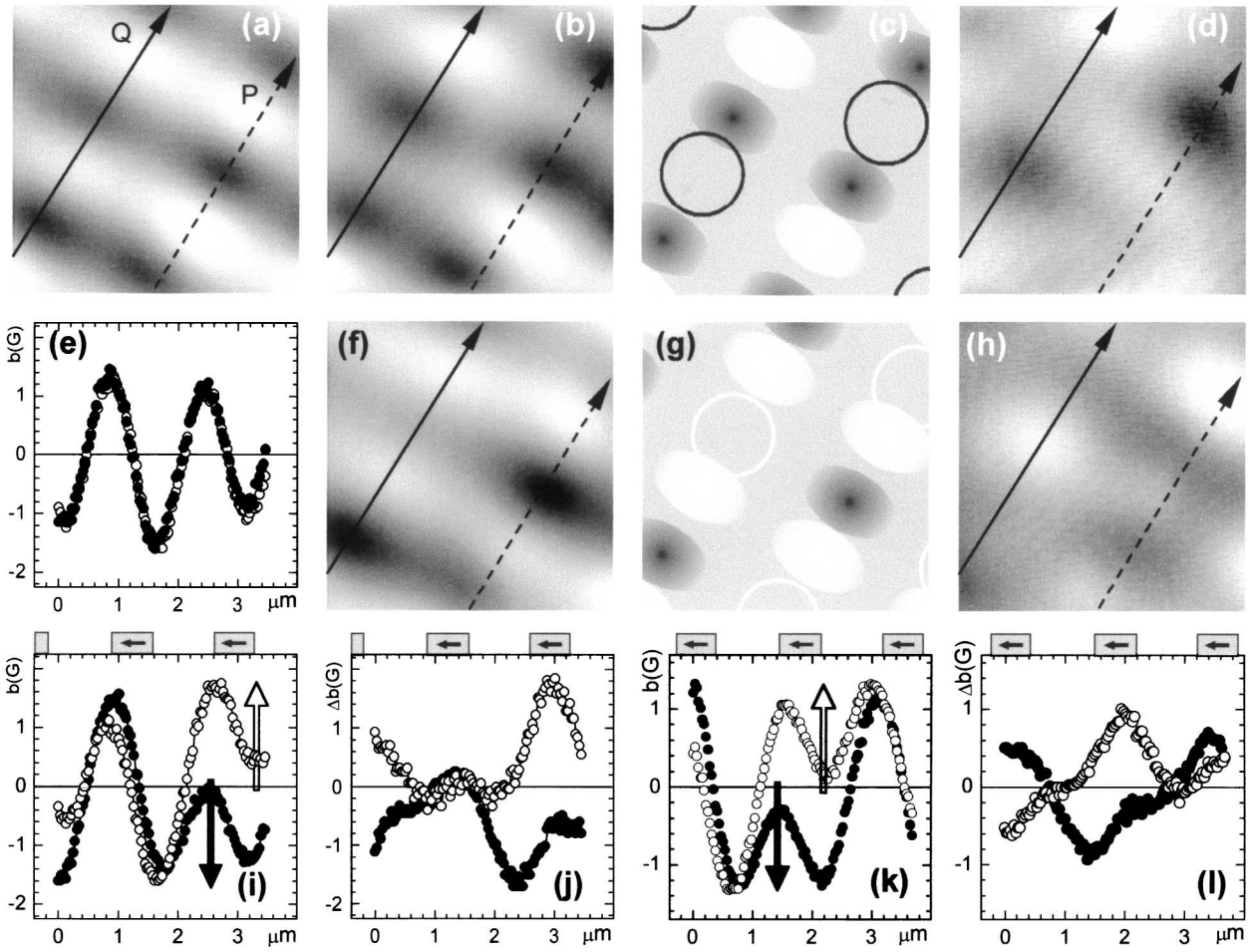

FIG. 3. SHPM images (a) at $T = 7.5$ K $> T_c$ and $B/B_1 = -\frac{1}{2}$; (b) at $T = 6$ K $< T_c$ and $B/B_1 = -\frac{1}{2}$; (d) image after subtracting (a) from (b); (f) image at $T = 6$ K and $B/B_1 = \frac{1}{2}$; (h) image after subtracting the image at $T = 7.5$ K and $B/B_1 = \frac{1}{2}$ [not shown, similar to (a)] from (f). All images are taken at the same position on the sample. (c) and (g) are schematic presentations of (b) and (f), respectively. The observed dipole fields are indicated and the FLs induced by the positive (negative) applied field are represented as white (black) circles. (e) Local field distribution at $T = 7.5$ K along arrow P in (a) for $B/B_1 = -\frac{1}{2}$ (filled symbols) and $B/B_1 = \frac{1}{2}$ (open symbols). (i) and (k) local field distribution at $T = 6$ K along arrows P and Q, respectively, at $B/B_1 = \frac{1}{2}$ (open symbols) and $-\frac{1}{2}$ (filled symbols). The white (black) arrow indicates the suggested position of the positive (negative) FL. (j) and (l) field distribution along arrows P and Q, respectively, after subtracting the dipole contribution, for $B/B_1 = \frac{1}{2}$ (open symbols) and $-\frac{1}{2}$ (filled symbols). The dot positions are indicated on the top axis of (i)–(l).

never perfect, dark spots can be clearly seen in Fig. 3(d), which can be associated with the negative FLs. A similar scenario occurs at $B/B_1 = \frac{1}{2}$ [Fig. 3(f)]; some of the negative (dark) poles in the image are completely suppressed because a positive FL is positioned on it [white circles in schematic drawing Fig. 3(g)]. After subtracting the dipole contribution at $T = 7.5$ K and $B/B_1 = \frac{1}{2}$ [not shown, but similar to Fig. 3(a)], the positive FLs can be observed as bright spots in Fig. 3(h). Both, for $B/B_1 = \frac{1}{2}$ and $-\frac{1}{2}$, one FL occupies each second magnetic dot, as can be expected from the magnitude of the applied field. A closer comparison of Fig. 3(a) and Figs. 3(d) and 3(h) reveals that each FL is not positioned in the center, but rather at a specific site, namely, on this pole where the dot-induced vortex has the opposite polarity of the FL. The perpendicular component of the local field, b, of the dots at $T = 7.5$ K $> T_c$ oscillates around $b = 0$ due to the succession of opposite magnetic poles [see line scans along arrow P in Fig. 3(e)]. Figures 3(i) and 3(k) show line scans of the total perpendicular component of the local field $b(x)$ along arrows P and Q, respectively, at $T = 6$ K and $B/B_1 = -\frac{1}{2}$ and $+\frac{1}{2}$. The position of the dots is indicated on the top axis. In Figs. 3(i) and 3(k), one can see that, due to the addition of a *positive* FL ($B/B_1 = \frac{1}{2} > 0$, open symbols) at the *negative* pole of a dot, no local field is left at this site, whereas in the case of an added *negative* FL ($B/B_1 = -\frac{1}{2} < 0$, filled symbols) the field at the *positive* pole is completely suppressed. This confirms our earlier statement that a *single* flux quantum is created at each pole, since the addition of a single opposite free FL at one of the poles leaves effectively no field at this site. Figures 3(j) and 3(l) show the same line scans as in Figs. 3(i) and 3(k) after subtraction

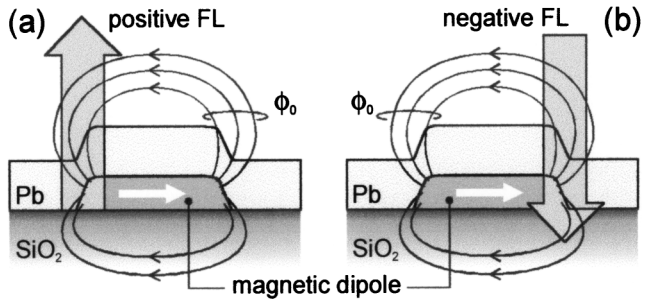

FIG. 4. Schematic presentation of the polarity dependent flux pinning, presenting the cross section of a Pb film deposited over a magnetic dipole with in-plane magnetization: (a) A positive FL (wide gray arrow) is attached to the dot at the pole where a negative flux quantum is induced by the stray field (black arrows), and (b) a negative FL is pinned at the pole where a positive flux quantum is induced by the stray field.

of the dipole signal of the dots. These line scans clearly show that the positions of the positive and the negative FLs are separated by about 0.6 μm, which is very close to the dot length and indicates that FLs of different polarity are *selectively pinned at the opposite ends of the dipoles,* as shown in Fig. 4. This pole selectivity implies that a free FL is attracted by the dot-induced antivortex in a similar way as it would be attracted by a normal free antivortex. This is reasonable since the flux and the current direction of the dot-induced antivortex have the same polarity as for a free antivortex. If the free FL is pinned at the pole of the dot and combines with the dot-induced antivortex, the total flux at this site will be completely annihilated [as was observed in Figs. 3(b), 3(f), 3(i), and 3(k)]. The circulating currents are however not completely annihilated; the remaining screening currents shield the stray field of the pole of the dot, leaving zero flux quanta threading the Pb film at this pole. The net result at this pole of the dot is that, instead of increasing the fluxoid to one flux quantum (as in the zero applied field case), a larger screening current is created in the opposite direction, which quantizes the fluxoid to zero flux quanta.

It should be mentioned that the interaction of free FLs with magnetic dipoles could be very different depending on the amount of stray field extruding from both sides of the dipoles. Not only the number of flux quanta created at the poles, but also the direction of the circulating screening currents that are generated to quantize the fluxoid at both poles depend crucially on the stray field strength. Only when the direction of these circulating currents corresponds to the sign of flux (as in a normal vortex), will the interaction between a free vortex and the dot-induced vortex be qualitatively (but not quantitatively) similar to normal vortex-vortex interaction.

In conclusion, we have used high resolution SHPM to investigate flux pinning in thin Pb films covering a square array of magnetic dipoles with in-plane magnetization. Fluxoid quantization of the Co dipole fields is observed when the sample is zero field cooled below T_c. Single flux quanta with opposite polarity are induced in the SC layer at the opposite poles of the dots and can be considered as an induced vortex-antivortex pair. The microscopic interaction of the FLs in a perpendicular applied field with these dot-induced flux quanta favors pinning of a FL at one specific pole of the magnetic dot. In our case, FLs are preferentially pinned at the pole where a vortex of opposite polarity was created. As a consequence of the broken field reversal symmetry, the pinned FL lattices are shifted with respect to one another depending on the polarity of the applied field.

The authors acknowledge M. Lange and H. J. Fink for fruitful discussions. This work is supported by the Fund for Scientific Research–Flanders (FWO), the Belgian IUAP, the Flemish GOA, and the ESF VORTEX programs, the British EPSRC and MOD Grant No. GR/J03077, and the University of Bath Initiative Fund. M. J. V. B. and K. T. acknowledge support from the FWO.

[1] M. Baert, V. V. Metlushko, R. Jonckheere, V. V. Moshchalkov, and Y. Bruynseraede, Phys. Rev. Lett. **74**, 3269 (1995).
[2] V. V. Moshchalkov, M. Baert, V. V. Metlushko, E. Rosseel, M. J. Van Bael, K. Temst, R. Jonckheere, and Y. Bruynseraede, Phys. Rev. B **54**, 7385 (1996).
[3] V. V. Moshchalkov, M. Baert, V. V. Metlushko, E. Rosseel, M. J. Van Bael, K. Temst, Y. Bruynseraede, and R. Jonckheere, Phys. Rev. B **57**, 3615 (1998).
[4] K. Harada, O. Kamimura, H. Kasai, T. Matsuda, A. Tonomura, and V. V. Moshchalkov, Science **274**, 1167 (1996).
[5] J. I. Martín, M. Vélez, J. Nogués, and I. K. Schuller, Phys. Rev. Lett. **79**, 1929 (1997).
[6] D. J. Morgan and J. B. Ketterson, Phys. Rev. Lett. **80**, 3614 (1998).
[7] M. J. Van Bael, K. Temst, V. V. Moshchalkov, and Y. Bruynseraede, Phys. Rev. B **59**, 14 674 (1999).
[8] I. F. Lyuksyutov and V. Pokrovsky, Phys. Rev. Lett. **81**, 2344 (1998).
[9] A. Oral, S. J. Bending, and M. Henini, Appl. Phys. Lett. **69**, 1324 (1996).
[10] A. Oral, J. C. Barnard, S. J. Bending, I. I. Kaya, S. Ooi, T. Tamegai, and M. Henini, Phys. Rev. Lett. **80**, 3610 (1998).
[11] For a magnetic dot with perpendicular magnetization, see I. K. Marmorkos, A. Matulis, and F. M. Peeters, Phys. Rev. B **53**, 2677 (1996).